"A Cochlear Nucleus Auditory prosthesis based on microstimulation"

Contract No. **No. NO1-DC-4-0005**
Progress Report #1

HUNTINGTON MEDICAL RESEARCH INSTITUTES
NEURAL ENGINEERING LABORATORY
734 Fairmount Avenue
Pasadena, California 91105

D.B. McCreery, Ph.D.
L.A. Bullara, B.S.
A.S. Lossinsky, Ph.D.

HOUSE EAR INSTITUTE
2100 WEST THIRD STREET
Los Angeles, California 90057

R.V. Shannon Ph.D
S. Otto M.S.
M. Waring, Ph.D

ABSTRACT

The objective of this project is to develop central auditory prostheses based on an array of microelectrodes implanted into the ventral cochlear nucleus, in order to restore hearing to patients in whom the auditory nerve has been destroyed bilaterally. Our contract calls for the development of arrays of silicon substrate electrodes, which should allow placement of many more electrode sites into the human ventral cochlear nucleus than is possible with discrete iridium microelectrodes. We are developing an array for implantation into the human cochlear nucleus which has 16 electrode sites distributed on 4 silicon shanks extending from an epoxy superstructure that is 2.4 mm in diameter.

One cat (CN149) has been implanted with one of these cochlear nucleus arrays for 75 days, as of this writing. We have made serial measurements of the neuronal responses (compound action potentials) evoked in the cochlear nucleus and recorded via electrode implanted chronically in the contralateral inferior colliculus. The thresholds of the response were quite stable between the 14th and 43rd day after the implant surgery, and ranged from less than 6 μA to about 14 μA. This is similar to the range of thresholds, and the post-implant threshold changes, that we have measured previously with discrete iridium microelectrodes implanted chronically in the cat cochlear nucleus and with previous chronically-implanted silicon substrate arrays. Overall, there was a slight tendency toward increasing threshold, which is consistent with the thickening of the gliotic capsule around the shanks.

In the same cat, we have demonstrated a method of determining the range of stimulus amplitudes over which adjacent electrode sites can activate separate neuronal populations that project into the contralateral inferior colliculus. The approach is a version of the paired-pulse interaction experiment in which the second pulse is applied within the absolute refractory of the neurons that might be excited by the first pulse. It allows for a very general definition of "information channel" in the lower auditory system, and is applicable to serial measurements in unanesthetized animals. As such, it complements the approach that we have used previously in which we measured the degree of spatial overlap of the neuronal activity evoked in the central nucleus of the inferior colliculus, when stimulating from different microelectrode sites in the CN, and where "channel" specifically designates a portion of the tonotopic projection of the cochlear nucleus into the inferior colliculus. Interaction between adjacent sites was measured over the stimulus range of 0 to 50 μA (0 to 4.5 nC/phase). A present, the stimulus used in the human patients implanted with the first-generation penetrating arrays is limited to 4 nC/phase. In cat CN149, the responses evoked from the adjacent sites on the array's caudal-lateral shank correspond most closely to the model for which there is no interaction between the adjacent electrode sites, over the full ranges of stimulus amplitude (0 to 50 μA, with a pulse duration of 90 μs per phase). This shank was shown at the time of surgery to be in the posteroventral cochlear nucleus. Across all of the shanks, there was the least interaction between the 2nd and 3rd sites, which are approximately 1.2 and 1.5 mm below the surface of the nucleus.

We have completed the design and construction of a unified 16-channel stimulating and recording system that will allow efficient measurements of the spatial profile of the neuronal activity evoked in the inferior colliculus while stimulating at the various sites in the cochlear nucleus. This system and its associated software can simultaneously record unit activity and compound action potentials. When used in conjunction with the method described in this report, we should have a more complete picture of how electrode sites and shanks with various separations can access separate information channels out of the feline cochlear nucleus.

INTRODUCTION

We are developing a silicon-substrate array for implantation into the human cochlear nucleus that has 16 electrode sites distributed on 4 silicon shanks extending from an epoxy superstructure that is 2.4 mm in diameter. This is the same footprint as our first- generation human arrays employing discrete iridium microelectrodes and is designed to be implanted using the same inserter tool. Figure 1A shows one of the dual-shank probes. The iridium electrode sites are located at depths of 0.8, 1.2, 1.5 and 1.8 mm below the probe spine. This will be their approximate depth below the dorsolateral surface of the cat's cochlear nucleus. Figure 1B shows an array with 2 of the probes (4 shanks and 16 electrode sites) extending from an epoxy superstructure that floats of the surface of the cochlear nucleus. The cable is directed vertically, to accommodate the transcerebellar approach to the feline cochlear nucleus.

To date, 10 of the silicon arrays have been implanted into 6 young adult female cats with normal hearing. The most recent implant (CN149) was made during the first quarter of this new contract.

METHODS

The arrays are implanted using aseptic surgical technique and general anaesthesia. The cat's scalp is opened in a midline incision, and the muscles reflected. A small craniectomy is made over the right occipital cortex and the bipolar recording electrode is introduced into the rostral pole of the right inferior colliculus. The reference electrode is slightly dorsal to the colliculus. These electrodes are solid 100 μm ss wire, with ~ 1 mm of the Teflon insulation removed for the tips. The recording electrode was inserted at the extreme rostral-medial margin of the IC, so as not to interfere with the mapping studies that are conducted just before the animal is sacrificed.

To access the cochlear nucleus, a craniectomy is made over the left cerebellum, extending up to the tentorium. The rostrolateral portion of the left cerebellum was then aspirated using glass pipettes. The electrode array was held by a partial vacuum onto the end of a metal inserter tube, and advanced into the cochlear nucleus. In cat CN149, the array was inserted into the cochlear nucleus with the shanks about 45^{o} from the vertical. This is intended to be a compromise between a mode in which the underside of the array will lie flat on the dorso-lateral surface of the nucleus, but will still allow the silicon shanks to traverse the isofrequency lamina.

Before releasing the vacuum, the array cable was fixed to the bone at the margin of the craniectomy, using medical grade SuperGlue and the cavity was filled with gelfoam.

RESULTS

Stability of the evoked responses

Figures 4A & 4B show the RGFs of the response evoked from the electrode sites on the caudal-lateral shank in cat CN149, at 14 and 43 days after implanting the array. These, and all of the physiologic data described in this report, were acquired with the cat un-anesthetized and supported on a technician's lap. Figures 5A,B, 6A,B, and 7A,B show the responses from the sites on the other 3 shanks. Overall, there was a decrease of about 50% in the amplitude of the action potentials between the 14th and 43rd day, but because the decrease was consistent for all stimulating sites and the threshold of the responses was quite

constant (Table 1), we attribute this decrease in amplitude to a problem with the recording electrodes, most likely to electrical leakage around the field joints that are buried in bone cement near the percutaneous connector. The thresholds of the response were quite stable between the 14th and 43rd day and ranged from less than 6 μA to about 14 μA (Table 1). This is similar to the range of thresholds that we have measured previously with discrete iridium microelectrodes implanted chronically in the cat cochlear nucleus and with previous chronically-implanted silicon substrate arrays. Overall, there was a slight tendency toward increasing threshold, which is consistent with the thickening of the gliotic capsule around the shanks.

Table I Thresholds of compound actions potentials, cat CN149

Shank	Site	Threshold (μA) day 14 after implant	Threshold, μA day 43
caudal-lateral	3	6	6
	7	6	6
	11	6	8
	15	8	8
caudal-medial	4	6	6
	8	<6	6
	12	8	12
	16	8	8
rostral-lateral	1	<6	<6
	5	<6	<6
	9	<6	8
	13	6	6
rostral-medial	2	14	14
	6	14	14
	10	6	12
	14	6	6

Interaction of stimulating electrode sites

Previously, we have demonstrated the capacity of the silicon probes to selectively activate different portions of the tonotopic gradient in the ventral cochlear nucleus by

performing current source-sink density analyses of the compound action potentials recorded at a regular sequence of depth in the contralateral inferior colliculus. In this report, we described a complimentary approach in which we determine the range of stimulus amplitudes over which adjacent electrode sites can activate separate neuronal populations that project into the contralateral inferior colliculus. The approach is a version of the paired-pulse interaction experiment in which the second pulse is applied within the absolute refractory of the neurons that might be excited by the first pulse. It is adapted from a scheme used by Liang et al (1991) to evaluate the selectivity of stimulating electrodes implanted in the sciatic nerve of the frog. Figure 8A illustrates the protocol. The first biphasic current pulse, each phase 90 μs in duration, is applied to the upper (shallower) of 2 adjacent electrode sites on the same silicon shank (See figure 1A). The second pulse begins 20 μs after the end of the anodic phase of the first pulse, and thus is delayed by 200 μs relative to the start of the first pulse.

It is first necessary to demonstrate that the second pulse occurs within the absolute refractory period of the first pulse, for the neurons in the feline cochlear nucleus. Figure 8A shows the response growth function for the first component of the response recorded in the contralateral inferior colliculus of cat CN149, when only the first pulse, and also when both pulses, are delivered through the same electrode site. Also shown is the amplitude of a response that simulates the condition of no interaction between the first and second pulses (no refractory behavior). This was obtained by adding the response to the first pulse to itself, after time-shifting the latter by 200 μs. The response to the double pulse (joint response) is indistinguishable from the response to the first pulse alone, demonstrating that neurons stimulated by the first pulse were completely refractory to the second pulse.

Figure 8C illustrates the situation wherein the first and second pulses are applied to adjacent electrode sites (in this case, to sites 5 & 9 on the rostrolateral shank of the array in cat CN149). The upper two traces are the responses when the sites were pulsed separately at 50 μA. The third trace was generated in the computer by shifting forward by 200 μs the response to pulsing site 9 alone and adding this shifted response to the response from pulsing site #5 alone (upper trace). It represents the condition of linear additivity, wherein there is no interaction and between the first and second pulses. Figure 8B implies that this is the condition when there is no overlap of the neural populations in the Cochlear nucleus that are excited from the 2 electrode sites. The lower trace In figure 8C is the response when the first pulse was applied to site 5 and the second (delayed) pulse was applied to site 9. The RGF's described below all were generated from the 1st component of these compound responses, or from the late component, as illustrated on the lower trace of figure 8C. From its short latency after the stimulus, the 1st response probably represent neurons activity evoked in direct pathway(s) from the CN to the IC, or through at most a single synapse. The larger, late component, with a latency of about 3 ms, probably represent neuronal activity evoked in the IC after transmission through at least 1 additional synapses. The computations based on the early component probably yield the most general definitions of independent neural projections from each electrode site in the cochlear nucleus into the contralateral IC. However, the analysis based on the late component can provide some insights as to how independence is maintained or reduced, after some neural processing in the IC. We note here that the late component was used in the current-source-sink analyses described in our earlier reports.

Figure 9 shows the RGFs for the caudal-lateral shank, which at the time of surgery was determined to be in the posteroventral cochlear nucleus. Figures A,B,C show the results for the early component of the CAP and figures D.E,F for the late component. Figure 9A shows the data for the shallowest pair of sites (0.8 and 1.2 mm below the dorsolateral surface of the

CN), figure 9B the next deepest pair (1.2 and 1.5 mm deep) and figure 9C the deepest pair (1.5 and 1.8 mm deep). Each graph shows the RGFs from 2 adjacent electrode sites when they are pulsed individually. Also plotted is the simulated condition of no site interaction, and the actual joint response when both sites are pulsed. For the joint response, the deeper of the two sites received the second (time-delayed) stimulus pulse.

On the caudal-lateral shank, across the full range of stimulus amplitudes, the joint response when sites #3 and #7 were pulsed together (Figure 9A), and also the joint response when sites #7 and #11 were pulsed together (Figure 9B) is identical to the plot of the model of no interaction between the sites. For sites #11 and #15 (Figure 9C), these plots diverge very slightly at the highest stimulus amplitude, indicating a small amount of interaction of the neuronal populations. Overall, the adjacent sites on this shank showed the least interaction over the full range of stimulus amplitudes.

As might be expected, there is slightly more interaction between the neural activity evoked from the adjacent sites on the caudal-lateral shank when the computation is based on the late component (Figure 9D,E,F). However, the degree to which the neuronal activity from the adjacent sites remains segregated even after one or two additional synapses, is quite remarkable.

For the other shanks, there was various amounts of interaction between the adjacent sites. On the caudal-medial shank (Figure 10), the plots of the joint response for sites #4 and #8 (Figure 10A) diverge from the plot simulating no interaction as the stimulus amplitude increased, indicating increased interaction of the neuronal population excited from these 2 sites. It is notable that electrode site 4 (0.8 mm below the surface) probably is in the DCN, while site 8 (1.2 mm below the surface) probably is in the PVCN, a reminder that with electrical stimulation, functional difference is no protection against overlap of stimulation. The plot of the joint response from sites #8 and #12 (Figure 10B) corresponds closely to the plot simulating no interaction, over the full range of stimulus amplitudes. The response from the deepest pair of sites (sites #12 and #16, Figure 10C) illustrates a limitation of this method of estimating interactions. The response evoked from electrode #16 was small and was sufficiently time-shifted relative to that of the response from electrode #12, such that the plot simulating no interaction is essentially identical to the response to pulsing electrode #12 alone.

Figure 11 shows the data from the rostral-lateral shank. For the early component of the CAP (Figure 11A,B C) the plot of the joint response from the shallowest pair of sites (sites #1 and #5, Figure 11A) begins to diverge from the plot simulating no interaction when the current pulse amplitude exceeded 25 μA, while sites #5 and #9 show a small amount of interaction only at the highest stimulus amplitude. For these sites, the data from the late component (figure 11D, E) is show the same. For the deepest pair of sites (sites #9 and #11, Fig. 11C, 11F), there was considerable interaction over most of the range of stimulus amplitudes, and for the late component, there was virtually 100% interaction over the entire range of stimulus amplitudes.

On the rostral-medial shank (Figure 12), the joint response from the 2 shallowest sites (sites #2 and #6, Figure 12A) indicates interaction between the sites when the pulse amplitude exceeded 30 μA. However, the plot of the joint response from sites #6 and #10 follows the plot simulating no interaction, up to the highest stimulus amplitude.

Figure 12C illustrates an interesting phenomena. The joint response from sites #10 and #14 is identical to the response when site #10 was pulsed alone, yet site #10 was pulsed 200 μs before site #14. This appears to be a physiological analog of “backward masking”, but the mechanism remains unclear. This situation might occur if the deeper sites (#14) were to

excite the axons that also are excited from site #10, before the arrival of the volley of action potentials from site #10, leaving these refractory and effectively blocking the volley from site 10. However, for this to occur in spite of the action potentials from site #10 having a 200 μs "head start", the axons from site #10 would have to have a conduction velocity of less than 1 meter/sec. It may be that the deep site excites the efferent axons directly, rather than via the somas or dendritic fields. Whatever the mechanism, the neurons excited from site 10 appear to be a subset of those excited from site, over all or most of the range of stimulus amplitudes.

DISCUSSION

The method used in this report to estimate the degree of interaction between the neuronal populations excited from adjacent electrode sites in the CN, allows for a very general definition of "information channel" in the lower auditory system. As such, it complements the approach that we have used previously in which we measured the degree of spatial overlap of the neuronal activity evoked in the central nucleus of the inferior colliculus, when stimulating from different microelectrode sites in the CN. In that experiment, "channel" specifically designates a portion of the tonotopic projection of the cochlear nucleus into the inferior colliculus. It is notable, however, that the late component of the CAP which was used in the present report is the same component used previously in the current source-sink analyses. The method described in this report requires only a single recording electrode at the edge of the inferior colliculus, and thus is applicable to chronic studies, and for data acquisition with the animal subject un-anesthetized.

The method does have some limitations. Thus, while the condition of no interaction of a neuronal population can be defined explicitly, the complementary condition of total interaction, in which the neurons activated from one electrode are a subset of the neurons activated from the other electrode, is more difficult to define and may depend upon the particulars of the neural substrate. Figures 8B & 12C illustrate 2 quite different outcomes. The absence of a reference for the condition of full interaction makes it difficult to quantify the degree of partial interaction when the model departs from the condition of no interaction. Finally, the compound action potentials from each electrode must be least roughly of the same amplitude and phase, so that the plot of the model for no interaction will differ substantially from the condition where the electrode sites pulsed individually. Figure 10C illustrates a situation in which this condition is not met. However, in most cases, the plots were well separated and the joint responses matched the model of no interaction, either perfectly or very closely, over at least a substantial portion of the range of stimulus amplitude.

We have completed the design and construction of a unified 16-channel stimulating and recording system that will allow efficient measurements of the spatial profile of the neuronal activity evoked in the inferior colliculus while stimulating at the various sites in the cochlear nucleus. This system and its associated software can simultaneously record unit activity and compound action potentials. When used in conjunction with the method described in this report, we should have a more complete picture of how electrode sites and shanks with various separations can access separate information channels out of the feline cochlear nucleus.

The cat CN149 remains alive and healthy, and so the precise anatomical locations of the electrode sites in the cochlear nucleus is yet to be determined. However, the data does illustrate the that capacity of the electrode sites to activate independent population of neurons is strongly dependent not only upon the stimulus amplitude but also on the location of the electrode sites in the cochlear nucleus. Overall, the joint responses from the adjacent sites on the caudal-lateral shank corresponded most closely to the model for no interaction across the full range of stimulus amplitudes, both for the early and the late component of the CAPs, and

at all depths in the nucleus. This shank was shown at the time of surgery to be in the posteroventral cochlear nucleus. Across all of the shanks, there was the least interaction between the 2nd and 3rd sites , which are 1.2 and 1.5 mm below the dorsolateral surface of the CN, as measured from the top of the shanks. (sites #7 & #11, #5 & #9, #8 & #12, #6 & 10). This was true both for the early and the late components. Over at least a portion of the range of stimulus amplitudes, these joint responses were identical to the model for no interaction. On the other three shanks, the joint response from the deepest pair of sites did not follow the model of zero interaction well, and on the rostral shanks, the joint responses from the deepes pair of sites were very similar to the responses from the deep site pulsed along, especially for the late component.

In the next contract quarter, we plan to supplement the data reported here from cat CN149 with measurements of the interaction of sites on adjacent silicon shanks. The study will terminate with an investigation of the spatial tuning of each site in the central nucleus of the inferior colliculus.

References

Liang, DH, Kovacs GT, Stormet CW and White RL (1991) " A method for evaluating the selectivity of electrodes implanted for peripheral nerve stimulation" IEEE Trans Biomed Engr 38:443-439

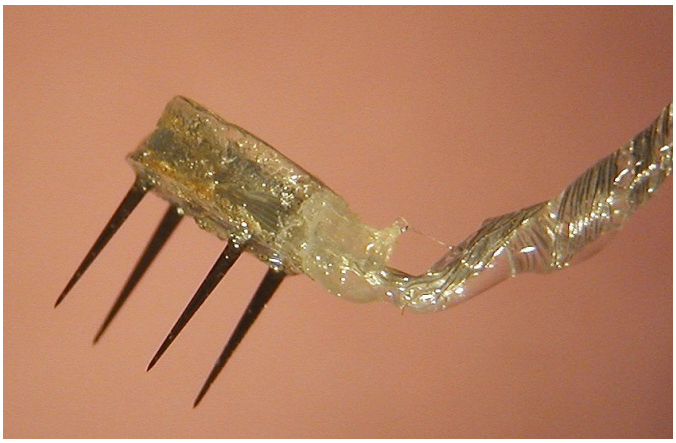

Figure 1A

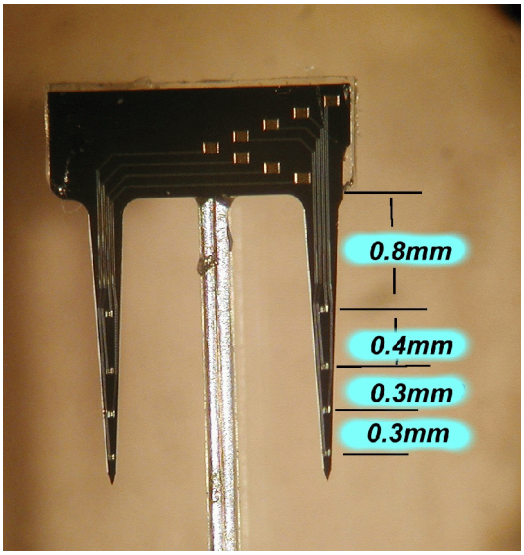

Figure 1B

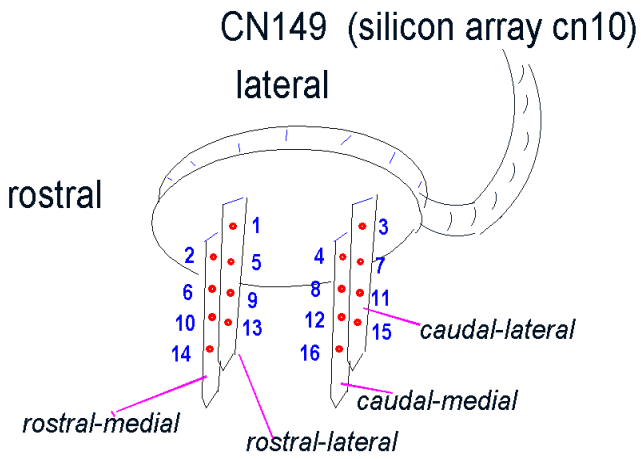

Figure 2

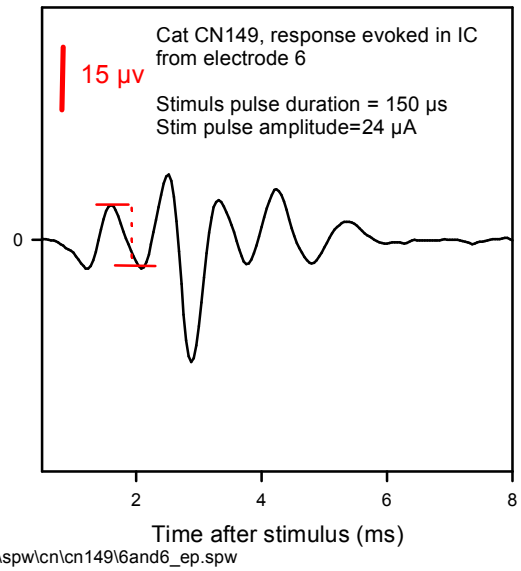

Figure 3

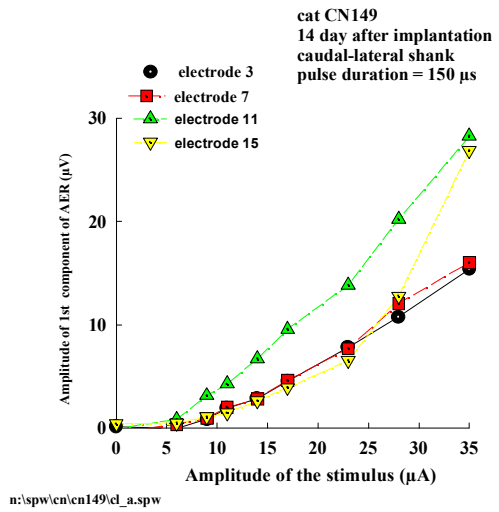

Fig 4A

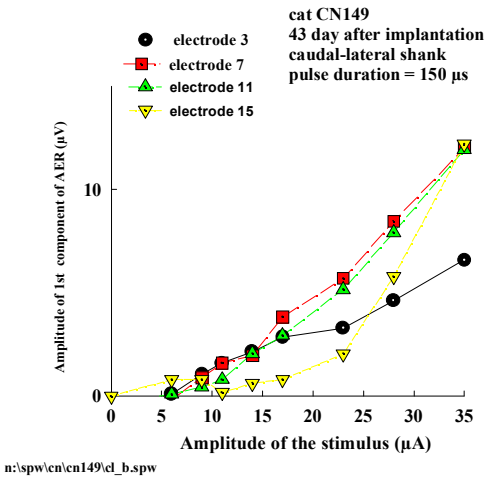

Fig 4B

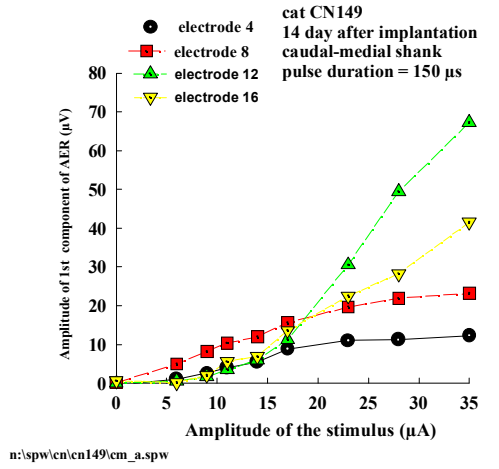

Fig 5A

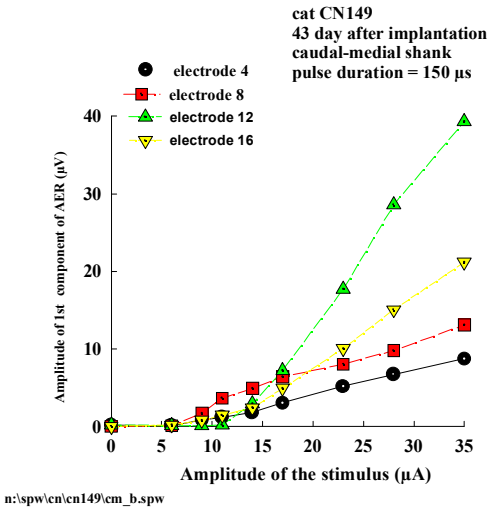

Fig 5B

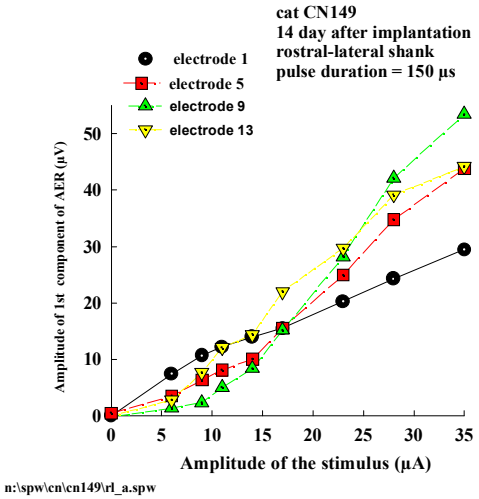

Fig 6A

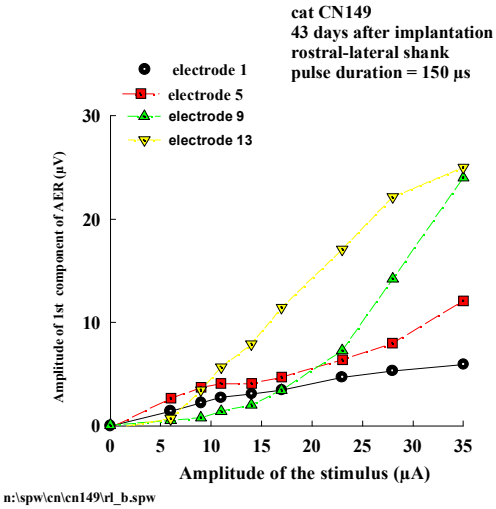

Fig 6B

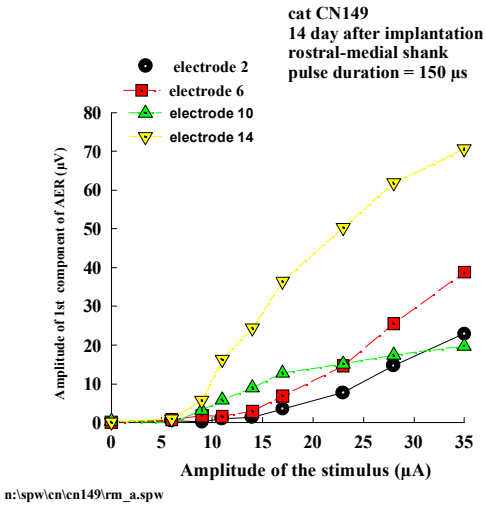

Fig 7A

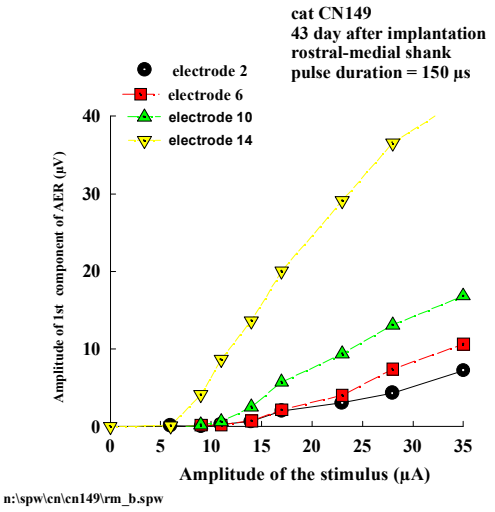

Fig 7B

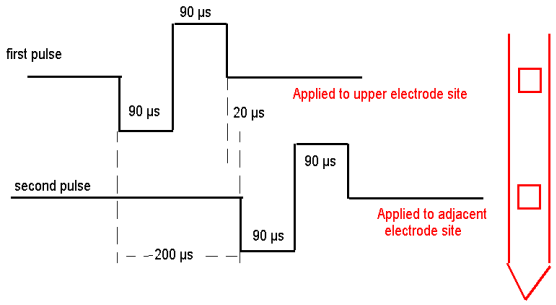
90 µs
first pulse
90 µs
20 µs
Applied to upper electrode site
90 µs
second pulse
Applied to adjacent electrode site
90 µs
200 µs

Fig 8A

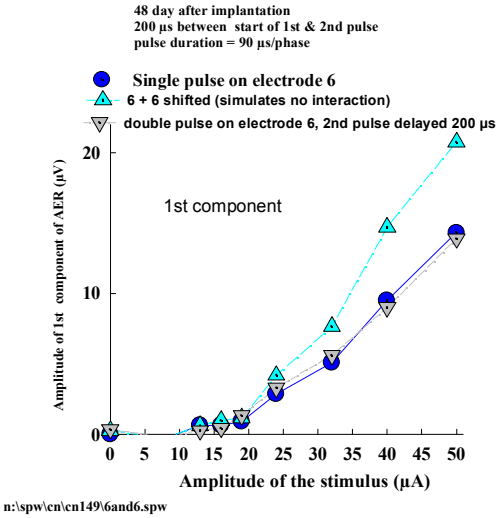
48 day after implantation
200 µs between start of 1st & 2nd pulse
pulse duration = 90 µs/phase
Single pulse on electrode 6
6 + 6 shifted (simulates no interaction)
double pulse on electrode 6, 2nd pulse delayed 200 µs
1st component
Amplitude of 1st component of AER (µV)
Amplitude of the stimulus (µA)
n:\spw\cn\cn149\6and6.spw

Fig 8B

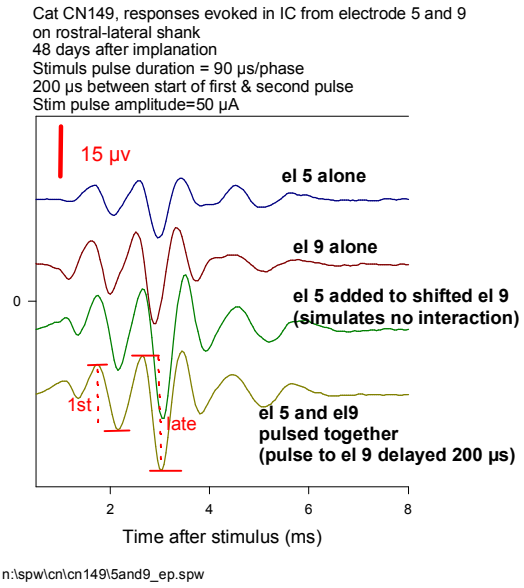
Cat CN149, responses evoked in IC from electrode 5 and 9
on rostral-lateral shank
48 days after implanation
Stimuls pulse duration = 90 µs/phase
200 µs between start of first & second pulse
Stim pulse amplitude=50 µA
15 µv
el 5 alone
el 9 alone
el 5 added to shifted el 9
(simulates no interaction)
1st
late
el 5 and el9
pulsed together
(pulse to el 9 delayed 200 µs)
Time after stimulus (ms)
n:\spw\cn\cn149\5and9_ep.spw

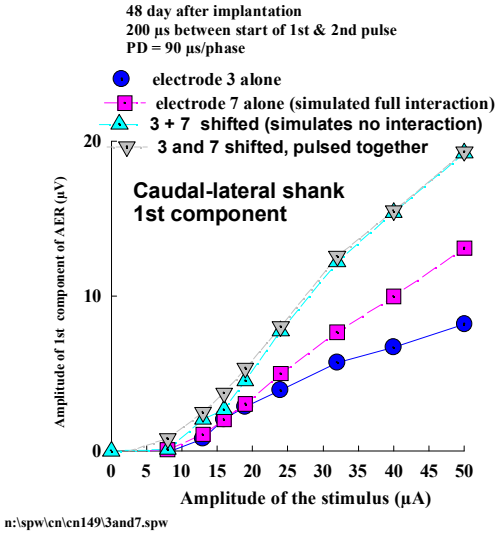

Fig 9A

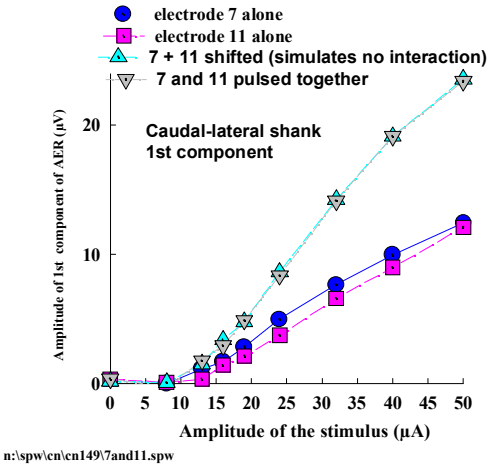

Fig 9B

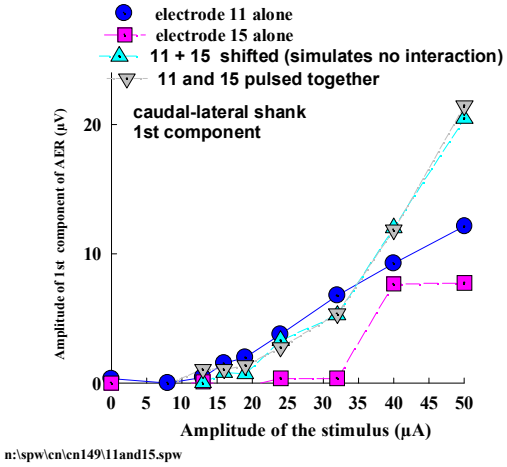

Fig 9C

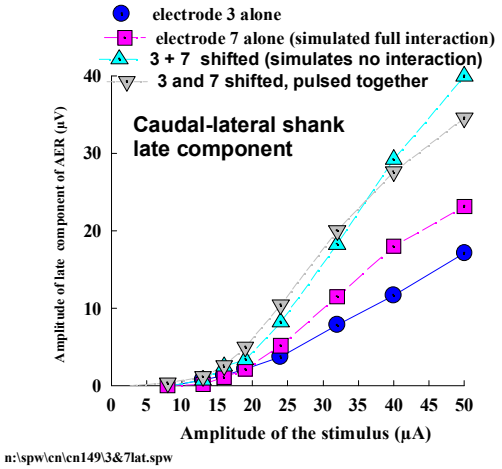

Fig 9D

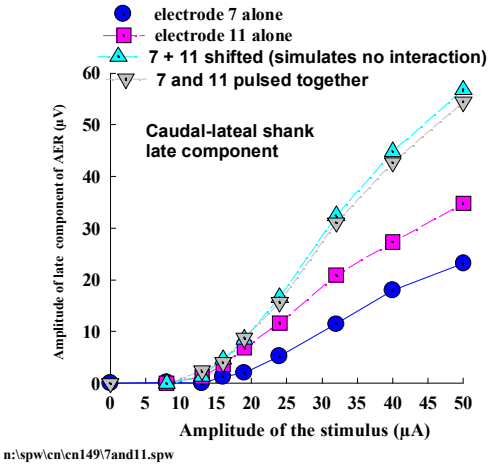

Fig 9E

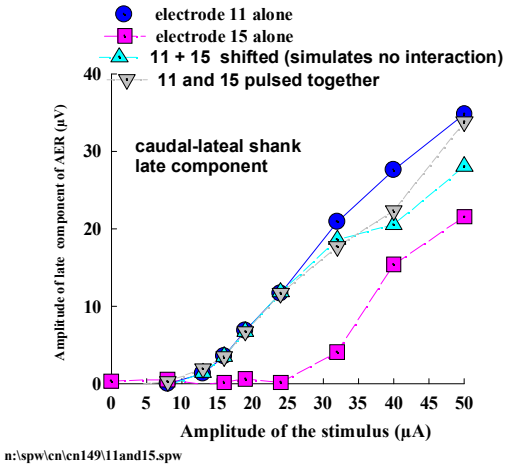

Fig 9F

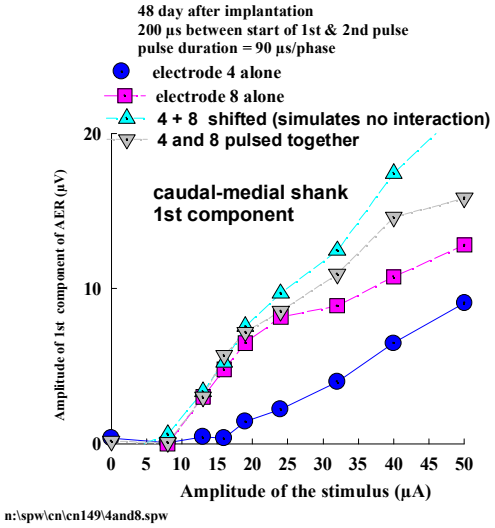

Fig 10A

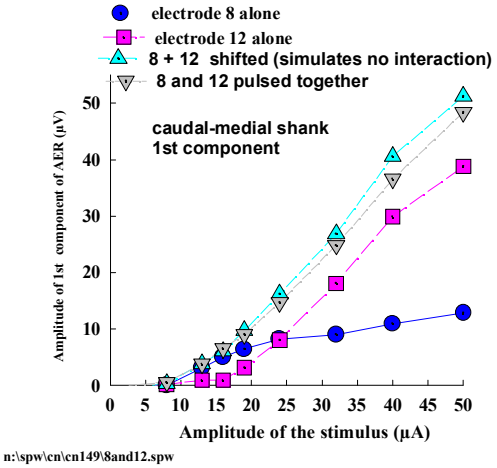

Fig 10B

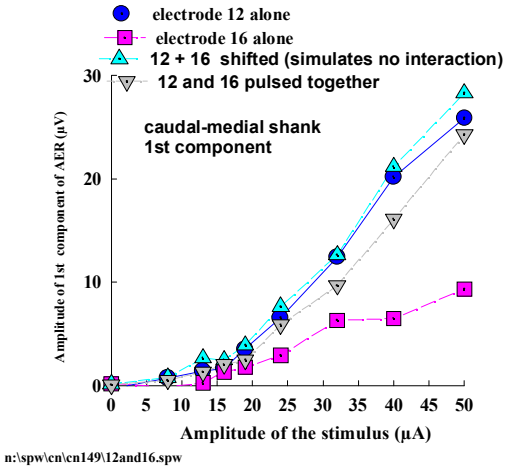

Fig 10C

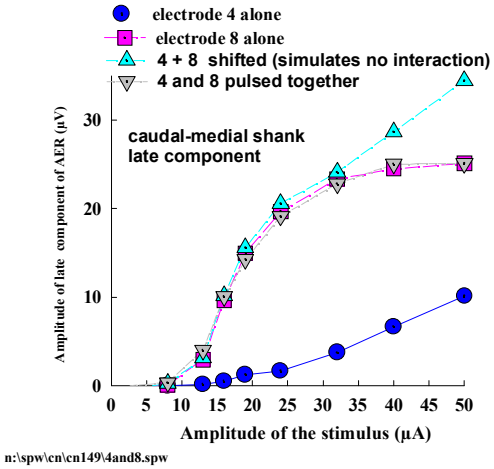

Fig 10D

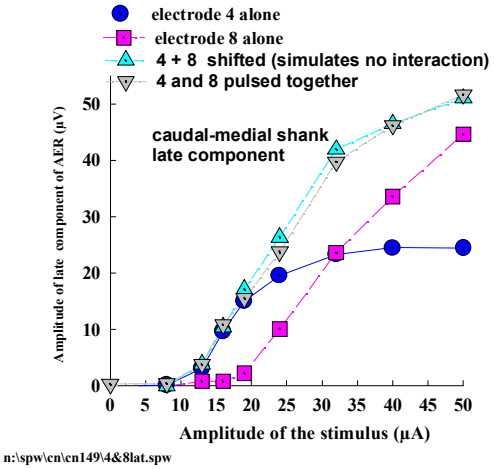

Fig 10E

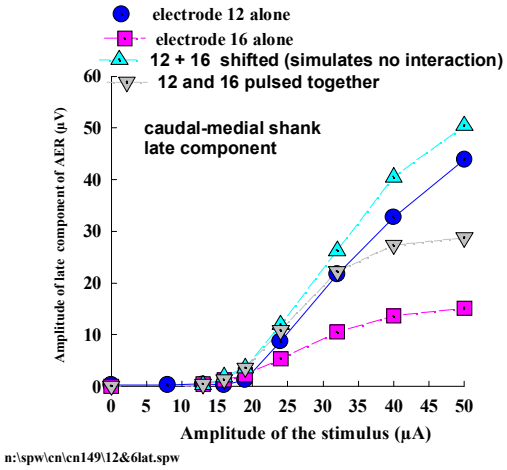

Fig 10F

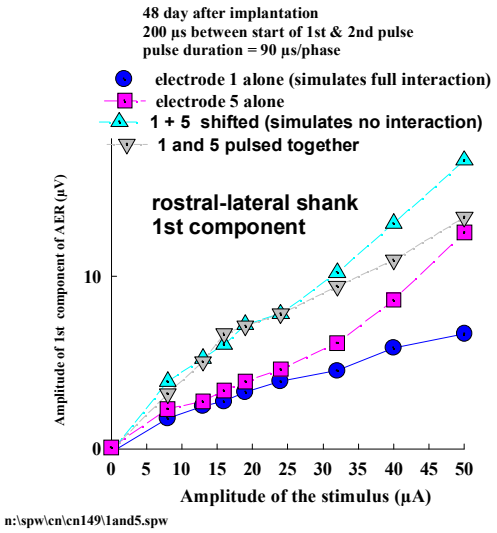

Fig 11A

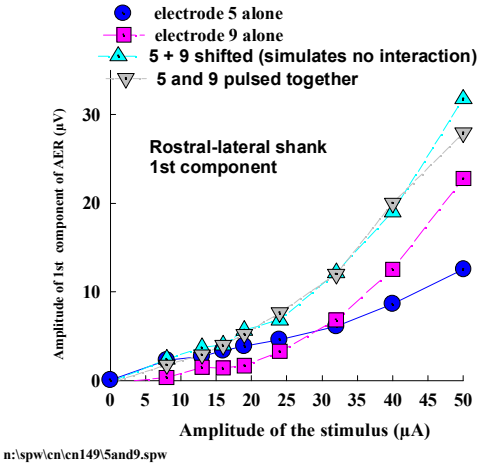

Fig 11B

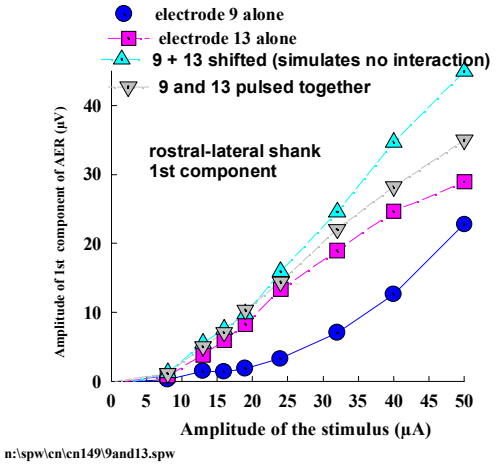

Fig 11C

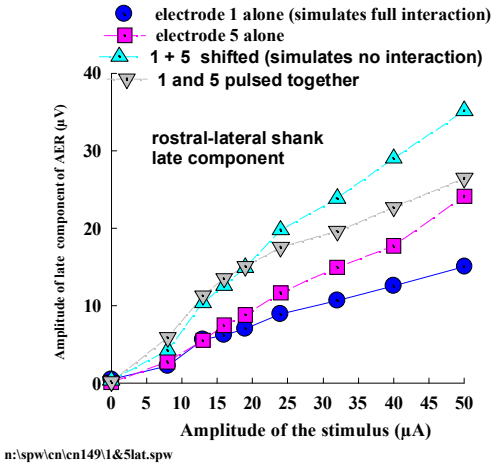

Fig 11D

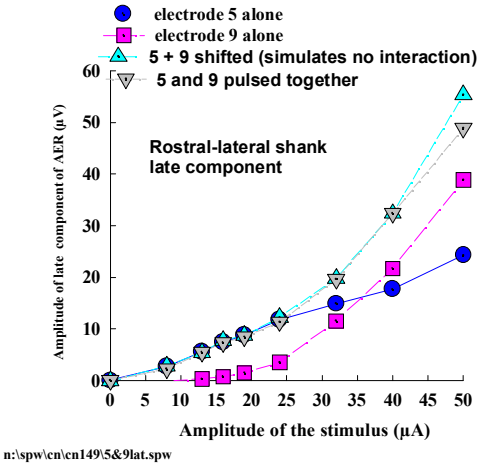

Fig 11E

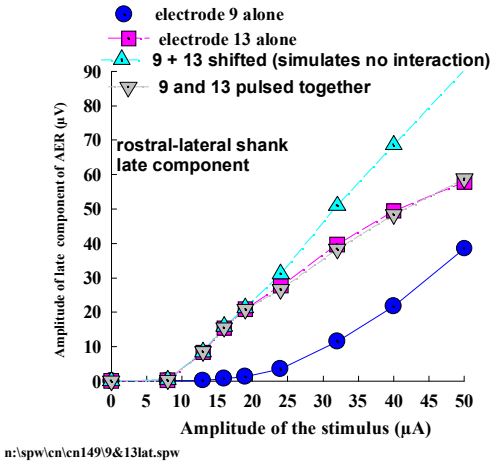

Fig 11F

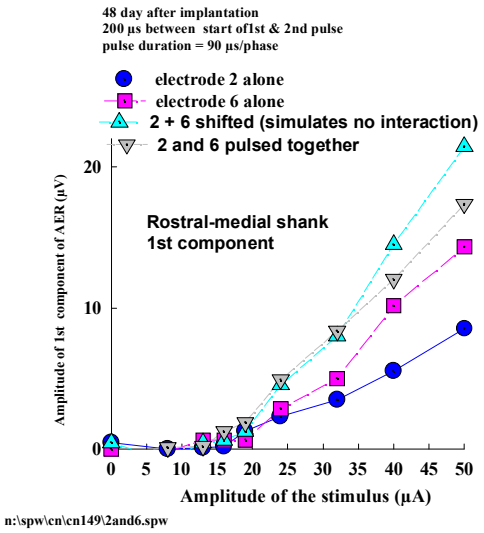

Fig 12A

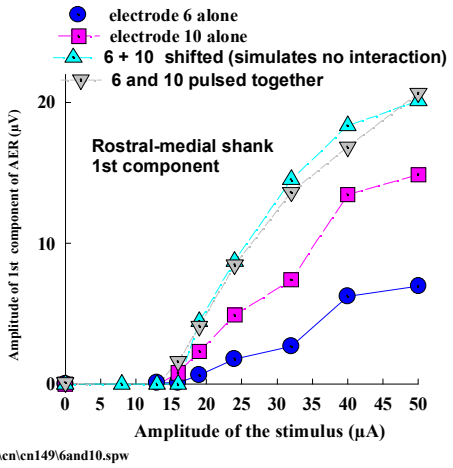

Fig 12B

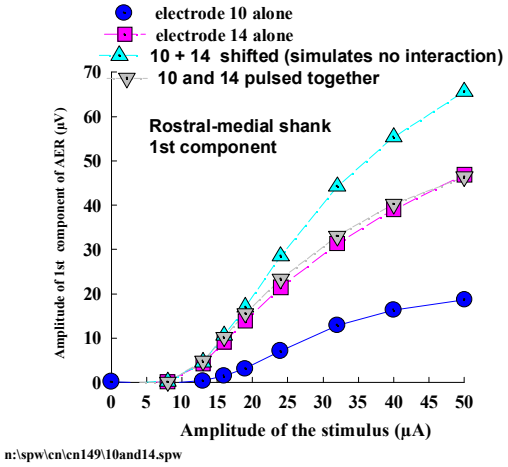

Fig 12C

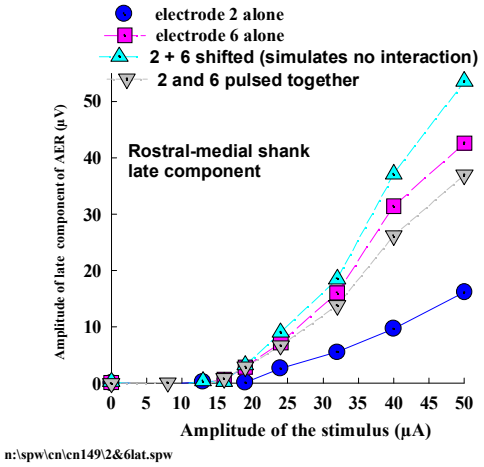

Fig 12D

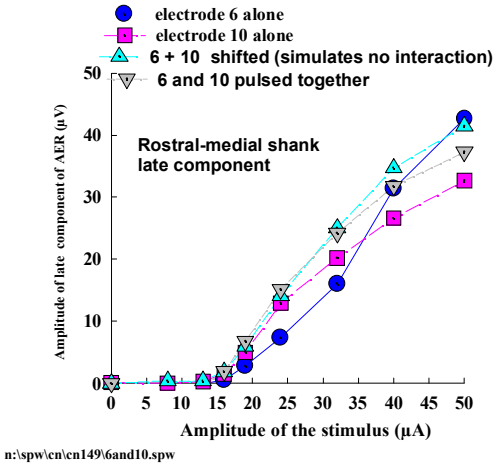

Fig 12E

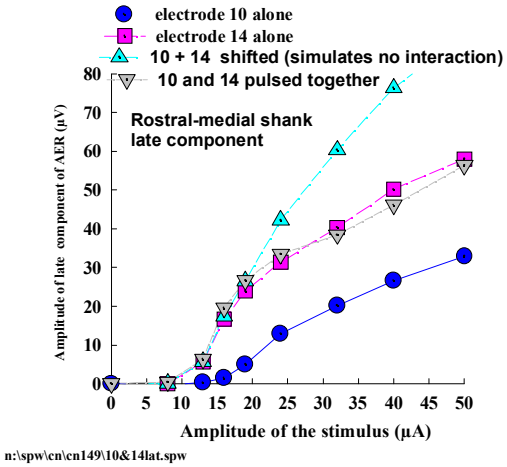

Fig 12F